Redox Biology 65 (2023) 102810

Contents lists available at ScienceDirect

Redox Biology

journal homepage: www.elsevier.com/locate/redox

Rapid phosphorylation of glucose-6-phosphate dehydrogenase by casein kinase 2 sustains redox homeostasis under ionizing radiation

Yilong Hao [a,1], Tao Ren [b,1], Xiaoke Huang [c], Mi Li [d], Jong-Ho Lee [e], Qianming Chen [a,**], Rui Liu [f,*], Qingfeng Tang [c,***]

[a] Stomatology Hospital, School of Stomatology, Zhejiang University School of Medicine, Zhejiang Provincial Clinical Research Center for Oral Diseases, Key Laboratory of Oral Biomedical Research of Zhejiang Province, Cancer Center of Zhejiang University, Engineering Research Center of Oral Biomaterials and Devices of Zhejiang Province, Hangzhou 310000, PR China

[b] Oncology Department (Key Clinical Specialty of Sichuan Province), The First Affiliated Hospital of Chengdu Medical College, Chengdu, 610500, PR China

[c] Department of Urology, Xindu District People's Hospital of Chengdu, Chengdu, 610500, China

[d] Department of Experimental Radiation Oncology, The University of Texas MD Anderson Cancer Center, Houston, TX, 77030, USA

[e] Department of Health Sciences, The Graduated School of Dong-A University, Busan, 49315, Republic of Korea

[f] State Key Laboratory of Oral Diseases, National Clinical Research Center for Oral Diseases, Research Unit of Oral Carcinogenesis and Management, Chinese Academy of Medical Sciences, West China Hospital of Stomatology, Sichuan University, Chengdu, Sichuan, 610041, PR China

ARTICLE INFO

Keywords:
G6PD
CK2
NADPH
Oxidative stress
Ionizing radiation

ABSTRACT

Exposure to ionizing radiation leads to oxidative damages in living cells. NADPH provides the indispensable reducing power to regenerate the reduced glutathione to maintain cellular redox equilibria. In mammalian cells, pentose phosphate pathway (PPP) is the major route to produce NADPH by using glycolytic intermediates, and the rate-limiting step of PPP is controlled by glucose-6-phosphate dehydrogenase (G6PD). Nevertheless, whether G6PD is timely co-opted under ionizing radiation to cope with oxidative stress remains elusive. Here we show that cellular G6PD activity is induced 30 min after ionizing radiation, while its protein expression is mostly unchanged. Mechanistically, casein kinase 2 (CK2) phosphorylates G6PD T145 under ionizing radiation, which consolidates the enzymatic activity of G6PD by facilitating G6PD binding with its substrate $NADP^+$. Further, CK2-dependent G6PD T145 phosphorylation promotes NADPH production, decreases ROS level and supports cell proliferation under ionizing radiation. Our findings report a new anti-oxidative signaling route under ionizing radiation, by which CK2-mediated rapid activation of G6PD orchestrates NADPH synthesis to maintain redox homeostasis, thereby highlighting its potential value in the early treatment of ionizing radiation-induced injuries.

1. Introduction

Ionizing radiation is a specific way by which energy travels, and it is powerful enough to ionize electrons from an atom, thus leading to the productions of ions. Exposure of living cells to ionizing radiation can rupture the chemical bonds of biological macromolecules, resulting in intensive chemical and biological changes [1]. In particular, radiolysis of cellular water produces the hydroxyl radical, and later superoxide and hydrogen peroxide as the subsequent products of reactive oxygen species (ROS) [2]. Water radiolysis elicited ROS production occurs within an extremely short period of time, thereby causing rapid oxidative stress that damages a wide spectrum of cellular components [3].

Nicotinamide adenine dinucleotide phosphate hydrogen (NADPH) functions as an essential electron donor in diverse reductive biochemical reactions, including the biosynthesis of proteins, nucleic acids and lipids [4]. Notably, NADPH provides the indispensable reducing power in the reaction to regenerate reduced glutathione (GSH), catalyzed by glutathione reductase, to tune cellular redox equilibria. GSH is the major antioxidant molecule for scavenging of cellular ROS in mammalian cells. Two GSH molecules provide two electrons to reduce hydrogen peroxide to water, and GSH are accordingly converted to form GSSG, which could be recycled back to GSH through accepting electrons from NADPH [5].

* Corresponding author.
** Corresponding author.
*** Corresponding author.
E-mail addresses: qmchen@zju.edu.cn (Q. Chen), liurui_scu@hotmail.com (R. Liu), tiantian77tom@yeah.net (Q. Tang).
[1] These authors contribute equally to this manuscript.

https://doi.org/10.1016/j.redox.2023.102810
Received 2 May 2023; Received in revised form 24 June 2023; Accepted 6 July 2023
Available online 7 July 2023

Therefore, failure in GSH regeneration due to the lack of NADPH makes cells vulnerable to oxidative damage.

The pentose phosphate pathway (PPP) is a fundamental metabolic process that utilize glucose to produce NADPH and 5-phosphate-ribulose, and the latter is used for the synthesis of pentose-containing molecules [6]. After glucose is converted to glucose-6-phosphate (G6P) by hexokinase, part of the intracellular G6P sheer off the glycolytic route towards tricarboxylic acid cycle, and shunt into PPP. Glucose-6-phosphate dehydrogenase (G6PD) is the rate-limiting enzyme that catalyzes the first step of PPP, converting G6P to 6-phosphogluconolactone, an irreversible reaction that determines the amount of G6P entering PPP [7]. Notably, through this reaction, G6P is oxidized by G6PD with the loss of electrons which are transferred to $NADP^+$ to produce NADPH [8]. 6-phosphogluconolactone is further processed by 6-phosphogluconolactonase and 6-phosphogluconate dehydrogenase to form the final product 5-phosphate-ribulose (R5P), which is the essential building block for generating nucleotides [9]. However, as the major source of NADPH production in mammalian cells, whether G6PD is timely regulated under ionizing radiation to modulate redox homeostasis remains largely unknown. In the present study, we show that casein kinase 2 (CK2) rapidly phosphorylates threonine (T)145 of G6PD in response to ionizing radiation, thereby enhancing the enzymatic activity of G6PD through facilitating the interaction between G6PD and its substrate $NADP^+$. In the irradiated cells, CK2-dependent G6PD T145 phosphorylation is required for NADPH production and maintaining redox homeostasis, and thereby support cell proliferation.

2. Materials and methods

2.1. Materials

G6PD pT145 antibody was customized from Boer Biotechnology (Chengdu, China). Antibodies recognizing GST (#2624), and CK2α (#2656) were purchased from Cell Signaling Technology. KU55933 (ab120637), and antibodies recognizing Tubulin (ab7291), Flag (ab205606), and G6PD (ab231828) were purchased from Abcam. [γ-^{32}P]-ATP was purchased from PerkinElmer (BLU002Z001MC). NU7441 (abx283114) was purchased from Abbexa. PD98059 (HY-12028) and AZD6738 (HY-19323) were purchased from MedChemExpress. SP600125 (S1460) and CX-4945 (S2248) were purchased from Selleckchem. Horseradish peroxidase-conjugated Goat Anti-Mouse antibody (511103) and horseradish peroxidase-conjugated Goat Anti-Rabbit antibody (511203) were purchased from ZenBio.

2.2. Cell culture and ionizing radiation

BEAS-2B cells were purchased from BIO Biotechnology (Chengdu, China). BEAS-2B cells were cultured with Dulbecco's Modified Eagle's Medium with 10% fetal bovine serum. HOK cell line was a gift provided by Dr. JS Gutkind (National Institute of Dental and Craniofacial Research, MD, USA). HOK cells were cultured with Keratinocyte Serum-Free Medium (Thermo Fisher Scientific, Inc.). Ionizing radiation was performed with an X-RAD 225 irradiator (Precision X-ray Inc., North Branford, CT) at the indicated doses.

2.3. Immunoprecipitation

Cells were lysed in a dish or well by using a buffer (0.1% SDS, 0.5 mM EDTA, 1% Triton X-100, 100 μM sodium pyrophosphate, 150 mM NaCl, 100 μM PMSF, 100 μM leupeptin, 1 μM aprotinin, 1 mM dithiothreitol, 100 μM sodium orthovanadate, 50 mM Tris-HCl [pH 7.5], and 1 mM sodium fluoride), and centrifugated at 13,000 g for 15 min. The precipitates were discarded, and the supernatants were mixed with indicated antibodies and rotated overnight at 4 °C, and then mixed with agarose beads and rotated for another 3 h. The precipitates were washed with phosphate-buffered saline (PBS) and analyzed by immunoblot.

2.4. Immunoblot analysis

Cells were lysed with a buffer (50 mM Tris, 1.0 mM EDTA, 150 mM NaCl, 0.1% SDS, 1% Triton X-100, 1% sodium deoxycholate, 1 mM PMSF), and centrifugated at 13,000 g for 10 min. The protein concentration in the lysate supernatant was quantified by the DC protein assay kit (Bio-Rad, 500–0121). 20 μL lysate supernatant containing about 50 μg protein was mixed with 5 μL 5 × reducing loading buffer (Beyotime, P0015), and boiled for 10 min. The samples were then loaded and analyzed by SDS-PAGE with a running buffer (25 mM Tris base, 192 mM glycine and 1 g/L SDS) at room temperature, and transferred to polyvinylidene difluoride membranes with a transfer buffer (25 mM Tris base, 192 mM glycine and 20% (v/v) methanol) on ice. Membranes were blocked with a blocking buffer (10 mM Tris (pH 7.4), 150 mM NaCl, 0.1% Tween 20, and 5% (v/v) bovine serum albumin) for 30 min at room temperature, and then incubated with the primary antibodies at 4 °C overnight at the following dilutions: anti-G6PD pT145 (1:1000), anti-GST (1:5000), anti-CK2α (1:1000), anti-Tubulin (1:2000), anti-Flag (1:5000), and anti-G6PD (1:1000). The blots were then washed and incubated with the secondary antibodies conjugated to horseradish peroxidase at room temperature for 2 h at the following dilution: Goat Anti-Mouse antibody (1:5000), and Goat Anti-Rabbit antibody (1:5000). The immunoreactivities were visualized by using the enhanced chemiluminescence reagents (Millipore, WBKLS0500).

2.5. Constructs and shRNAs

Human G6PD gene was cloned into pcDNA3.1/hygro(+)-Flag. QuikChange site-directed mutagenesis kit (Stratagene, La Jolla, CA) was used to introduce the indicated mutations. shRNAs were synthesized using the following sequences: G6PD shRNA, TTC TTA TAG CAG AGA GGC T (targeting non-coding region); CK2α (CSNK2A1) shRNA, TCA GGA GAC AGA TAG GGC C; control shRNA, GCT TCT AAC ACC GGA GGT CTT.

2.6. Preparation of recombinant proteins

The DNA of WT and mutant G6PD was cloned into pCold I vector. The DNA of CK2α was cloned in to pGEX4T-1 vector. Recombinant constructs were transferred into BL21(DE3) bacteria as previously described [10]. Expression of recombinant proteins was stimulated by addition of 0.5 mM isopropyl β-D-1-thiogalactopyranoside (IPTG). BL21 bacteria cells were then cultured in Lysogeny Broth medium for 16 h at 16 °C or 30 °C, followed by lysis with sonication.

For the purification of His-tagged proteins, the lysed bacterial samples were transferred to a Ni-NTA column (GE Healthcare Life Sciences). The column was flushed with 20 mM imidazole and the protein was eluted with 250 mM imidazole. For the purification of GST-tagged proteins, cell lysates were loaded onto a GSTrap HP column (GE Healthcare Life Sciences), washed with five column volumes of PBS, and eluted with 10 mM reduced glutathione. To remove the contaminants, the eluted samples were separated through a HiPrep 16/60 Sephacryl S-200 HR gel filtration column (GE Healthcare Life Sciences).

2.7. Measurement of G6P dehydrogenation activity

G6P dehydrogenation activity in cell lysates and immunoprecipitates was examined by using Glucose-6-Phosphate Dehydrogenase Activity Colorimetric Assay Kit obtained from BioVision (#K757-100). For the measurements using cell lysates sample, 2×10^5 cells were seeded in a well of 6-well plate, and incubated with fresh medium overnight. The cells were treated with ionizing radiation at indicated doses, and harvested at the indicated time points. The cell lysates were used for the measurement of G6P dehydrogenation activity. The value of G6P dehydrogenation activity was normalized to cell numbers. For the measurements using immunoprecipitates sample, 2×10^5 cells with

expression of Flag-G6PD were seeded in a well of 6-well plate, and incubated with fresh medium overnight. Cells were treated with ionizing radiation at indicated doses, and Flag-G6PD proteins were precipitated from the cell lysates 30 min after irradiation. The precipitates were used for the measurement of G6PD activity. The value of G6PD activity was normalized to the intensity of the bands corresponding to Flag-G6PD in the immunoblots.

2.8. In vitro kinase assay for CK2

Kinase reactions were performed as described previously [11]. Purified CK2α protein (10 ng) was incubated with purified G6PD protein (200 ng) in 25 μL kinase buffer (50 mM Tris-HCl, pH 7.5, 100 mM KCl, 5 mM $MgCl_2$, 1 mM Na_3VO_4, 50 μM DTT, 5% glycerol, 100 μM ATP) at 30 °C for 30 min. For *in vitro* kinase assay using [γ-^{32}P]-ATP, 10 μCi of the ^{32}P-labeled ATP was added in the reaction system. G6PD protein was precipitated and analyzed by SDS-PAGE, followed by immunoblot with indicated phosphorylation site-specific antibodies or autoradiography.

For *in vitro* kinase assay using ATPγS, the experiment was performed following the Kinase Reaction and Alkylation Protocol (Abcam) according to previous report [12]. Briefly, purified CK2α protein and G6PD protein were incubated with the reaction buffer (20 mM Hepes, pH 7.5, 100 mM NaCl, 1 mM ATPγS (ab138911, Abcam), 10 mM $MgCl_2$) for 30 min at 30 °C, followed by addition of 2.5 mM p-nitrobenzyl mesylate (ab138910, Abcam) to the reaction system and incubation at room temperature for another 1 h G6PD protein was then precipitated and analyzed by SDS-PAGE, followed by immunoblot with the thiophosphate ester specific antibody (ab92570, Abcam).

2.9. Measurement of G6PD binding with NADP$^+$

Cellular G6PD proteins or bacterially purified G6PD proteins were precipitated and incubated with binding buffer (50 mM Tris-HCl (pH 7.5), 1 mM $MgCl_2$, and 2.5 mM DTT) containing 0.1 mM NADP and 10 μCi [^{14}C]-NADP at 25 °C for 10 min. The protein-beads complexes were then washed with binding buffer for five times, and the radioactivity signal was detected by liquid scintillation counting. Data was normalized to the amounts of G6PD protein.

[^{14}C]-NADP was enzymatically synthesized using recombinant human NAD kinase obtained from BioVision (#7560) and [^{14}C]-NAD obtained from PerkinElmer (NEC831010UC), following previous report [13]. [^{14}C]-NAD (50 μCi) was incubated with a reaction buffer (100 μL of 0.5 M Tris/HCl, pH 7.5; 20 μl of 0.5 M $MgCl_2$; 240 μL of 10 mM ATP; 40 μL of 7.1 mM NAD; 60 μg of recombinant human NAD kinase). The reaction was performed at 37 °C for 120 min, and terminated by adding 1.0 mL ethanol to the mixture. The mixture was dried at 25 °C, redissolved in 1.0 mL water, centrifuged at 1000 g for 15 min to remove the insoluble substance. The supernatant fluid was dried at 25 °C, and redissolved in water.

2.10. Measurement of cellular ^{14}C–R5P

Measurement of cellular ^{14}C–R5P was performed by conversion of R5P to phosphoribosyl pyrophosphate and subsequent conversion of phosphoribosyl pyrophosphate to AMP, according to previous report [14]. Briefly, 20 μL cell lysate was added into 100 μL reaction buffer, containing 5 μM Tris-HCl, pH 7.4; 50 nM disodium EDTA; 250 nM reduced glutathione; 10 nM adenine; 1 μg bacterially purified phosphoribosyl pyrophosphate synthetase 1 protein; 1 μg bacterially purified adenine phosphoribosyltransferase protein; 100 nM ATP; 750 nM magnesium chloride; 4.2 μM sodium phosphate (pH 7.4), and the mixture was incubated at 37 °C for 60 min. The mixture was then applied to a cellulose thin layer chromatography sheet, and developed for 3 h in a solvent system containing butyl alcohol: acetone: glacial acetic acid: 5% ammonium hydroxide: water (7: 5: 3: 3: 2, vol/vol). The spot corresponding to the AMP marker was cut out and counted in a liquid scintillation counter. The level of ^{14}C–R5P was calculated as the difference of the amount of radioactive AMP generated in the presence and absence of phosphoribosyl pyrophosphate synthetase 1 protein.

2.11. Measurement of cellular levels of NADPH and NADP$^+$

2×10^5 cells with stable expression of indicated genes and/or shRNAs were seeded in a well of 6-well plate, and incubated with fresh medium overnight. Cells were treated with 12 Gy ionizing radiation, and measurement of cellular levels of NADPH and NADP$^+$ were performed 3 h after irradiation by using NADP/NADPH Quantification Colorimetric Kit obtained from BioVision (#K347-100), following the manufacture's introduction. The data was normalized to the total cell numbers.

2.12. Measurement of cellular oxidative stress

2×10^5 cells with stable expression of indicated genes and/or shRNAs were seeded in a well of 6-well plate, and incubated with fresh medium overnight. Cells were treated with 12 Gy ionizing radiation, and cellular oxidative stress was measured by the following methods 3 h after irradiation. The levels of GSH/GSSG ratio were determined using the GSH/GSSG Ratio Detection Assay Kit obtained from Abcam (ab138881) and quantified using a microplate reader (Ex/Em = 490/520 nm). The level of cellular DCFDA signal was measured by using Reactive Oxygen Species (ROS) Detection Assay Kit obtained from BioVision (K936-100) and evaluated by using a microplate reader (Ex/Em = 495/529 nm). The level of 8-OHdG was examined by using 8-hydroxy 2 deoxyguanosine ELISA Kit obtained from Abcam (ab201734). The data was normalized to the cell numbers.

2.13. BrdU cell proliferation assay

Cells were plated in 96-well plate at 2×10^5 cells/ml in 100 μL/well, and incubated with fresh medium overnight. Cells were treated with 12 Gy ionizing radiation. 12 h after indicated irradiation, BrdU incorporation assay was performed by using BrdU Cell Proliferation ELISA Kit (colorimetric) purchased from Abcam (ab126556), according to the manufacture's introduction. The data was normalized to the total cell numbers.

2.14. Colony formation assay

100 cells were seeded in a well of 6-well plates. After indicated irradiation or other treatment, cells were cultured for 14 days. The clones were fixed by incubation with methanol for 3 min, stained with crystal violet solution for 15 min and washed gently with PBS for 3 times. Those clones containing over 50 cells were selected and the number of clones were counted.

2.15. Quantification and statistical analysis

All data represent the mean ± SD of at least three independent experiments/samples unless otherwise specified. Statistical analyses were performed using two-sided Student's *t*-test for compassion between two groups. For those experiments containing three or more groups, ANOVA test was performed firstly. If the result of ANOVA test was significant ($P < 0.05$), *t*-test was then performed as the secondary test. If comparison between two groups (*t*-test) was performed more than one time with the same set of data, Bonferroni correction was used for the multiple hypothesis correction (requiring $P < 0.05/N$, N indicates the number of comparisons), to avoid reporting false positive results. In the figure legends, the P value was calculated from *t*-test unless otherwise specified.

3. Results

3.1. Ionizing radiation increases G6PD activity

To determine whether cellular G6PD activity is altered under ionizing radiation, human normal oral epithelial keratinocyte HOK cell line and human bronchial epithelial BEAS-2B cell line were utilized, as these cells were previously found to be radiosensitive [15,16]. After treated with 12 Gy ionizing radiation, the lysates of HOK and BEAS-2B cells were collected and examined, and it showed a 2.5~5-fold augment in the cellular G6P dehydrogenation activity (Fig. 1A). The enhanced cellular G6P dehydrogenation activity seems a quick response to ionizing radiation, evidenced by a time-course experiment that detected the initial increase at only 30 min post-irradiation (Fig. 1A). Additionally, treatment with 5–20 Gy radiation revealed a dose-dependent increase of cellular G6P dehydrogenation activity in both HOK and BEAS-2B cells (Fig. 1B).

To determine whether ionizing radiation evoked cellular G6P dehydrogenation activity through modulating cellular G6PD abundance, protein expression of G6PD was measured by immunoblot after multiple radiation treatments, and however, no apparent alteration was found (Fig. 1C–D). Strikingly, Flag-G6PD immunoprecipitates derived from irradiated HOK or BEAS-2B cells showed a substantially higher enzymatic activity, compared to the counterparts from non-irradiated cells (Fig. 1E). These data indicate that exposure to ionizing radiation rapidly activates G6PD by increasing its enzymatic activity.

3.2. CK2 phosphorylates G6PD T145 upon ionizing radiation

To explore the key factors involved in the ionizing radiation-induced G6PD activity, we inhibited a group of radiation-responsive proteins by incubating HOK cells with specific chemical antagonists in prior to exposure to ionizing radiation. Treatment with CK2 inhibitor CX-4945 largely eliminated ionizing radiation-induced G6P dehydrogenation activity (Fig. 2A). In contrast, incubation with KU55933 (ATM inhibitor), NU7441 (DNA-PK inhibitor), AZD6738 (ATR inhibitor), PD98059 (MEK/ERK pathway inhibitor) or SP600125 (JNK inhibitor) caused only negligible effects (Fig. 2A). CK2 kinase ubiquitously exists in diverse tissue and cell types, and has pivotal roles in the modulation of oxidative stress and radiation-related injuries [17,18]. Co-immunoprecipitation detected a weak interaction between endogenous G6PD and CK2α protein, the catalytic subunit of CK2 kinase, in the unirradiated HOK and BEAS-2B cells (Fig. 2B). Notably, the G6PD protein pulled down apparently more CK2α protein in the irradiated cells, indicating that ionizing radiation reinforced G6PD binding with CK2α (Fig. 2B). Further, bacterially purified His-G6PD protein could be precipitated by bacterially purified GST-CK2α protein, but not GST protein, in an *in vitro* system (Fig. 2C), indicating that G6PD can directly interact with CK2α.

CK2 functions as a pleiotropic signal transducer by phosphorylating the serine or threonine residue of more than three hundred proteins [19]. To verify whether G6PD is a new phosphorylation substrate for CK2, bacterially purified His-G6PD protein was mixed with purified GST-CK2α protein for an *in vitro* kinase assay, and [γ-^{32}P]-ATP was used

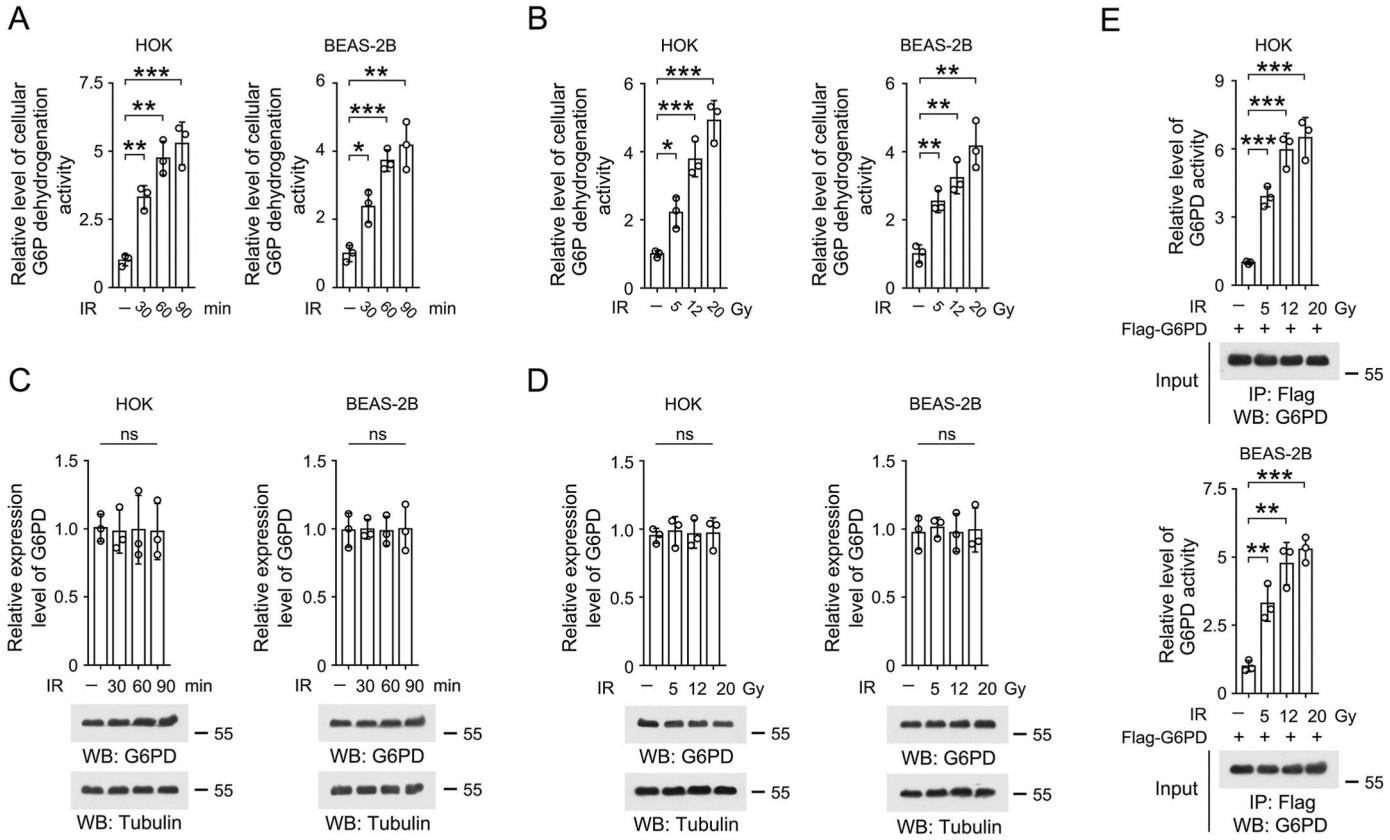

Fig. 1. Ionizing radiation increases G6PD activity (A) HOK and BEAS-2B cells were treated with 12 Gy ionizing radiation, and the G6P dehydrogenation activity in the cell lysates was measured at the indicated time after irradiation. IR, ionizing radiation. $^{*}P < 0.05$, $^{**}P < 0.01$, $^{***}P < 0.001$. (B) HOK and BEAS-2B cells were treated with ionizing radiation at indicated doses, and the G6P dehydrogenation activity in the cell lysates was measured 30 min after irradiation. $^{*}P < 0.05$, $^{**}P < 0.01$, $^{***}P < 0.001$. (C) HOK and BEAS-2B cells were treated with 12 Gy ionizing radiation, and the expression of G6PD was examined by immunoblot at indicated time after irradiation. The result of ANOVA test was not significant (ns, $P \geq 0.05$). (D) HOK and BEAS-2B cells were treated with ionizing radiation at indicated doses, and the expression of G6PD was examined by immunoblot 30 min after irradiation. The result of ANOVA test was not significant (ns, $P \geq 0.05$). (E) HOK and BEAS-2B cells with expression of Flag-G6PD were treated with 12 Gy ionizing radiation, and Flag-G6PD protein was precipitated 30 min after irradiation. The G6PD activity in the precipitates was measured. $^{**}P < 0.01$, $^{***}P < 0.001$.

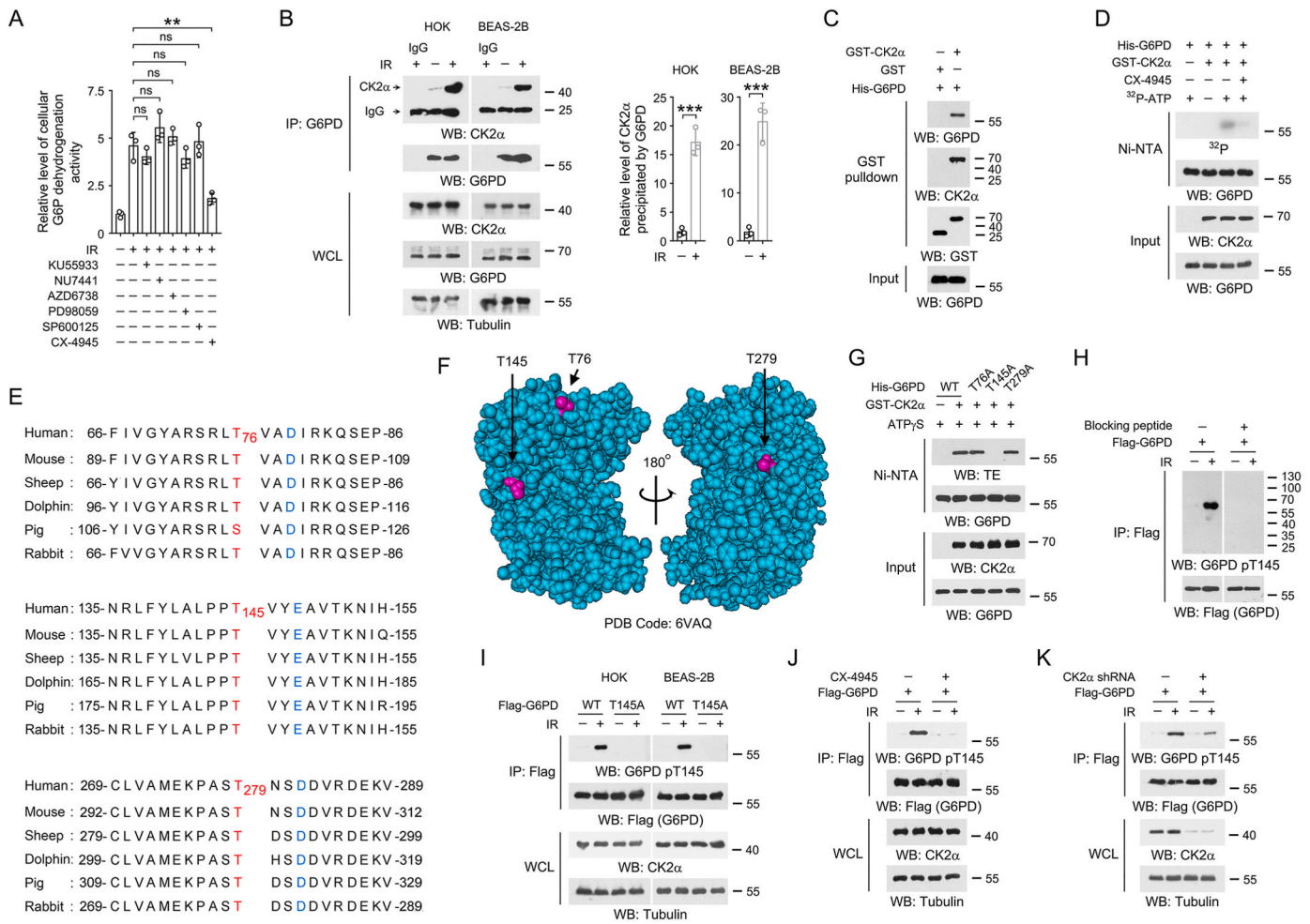

Fig. 2. CK2 phosphorylates G6PD T145 under ionizing radiation (B-D, G-K) Immunoblot analyses were performed using indicated antibodies.
(A) BEAS-2B cells were pre-treated with 10 μM KU55933, 1 μM NU7441, 2 μM AZD6738, 20 μM PD98059, 20 μM SP600125, or 15 μM CX-4945 for 2 h, and then cells were treated with 12 Gy ionizing radiation. Cellular G6P dehydrogenation activity was measured 30 min after irradiation. IR, ionizing radiation; $^{**}P < 0.01$; ns, not significant.
(B) HOK and BEAS-2B cells were treated with 12 Gy ionizing radiation, and cells were harvested 30 min after irradiation. Co-immunoprecipitations were performed using indicated antibodies (left panel). Co-immunoprecipitation experiments were repeated for three times, and the intensities of the immunoblot bands for the precipitated CK2α protein were analyzed. WCL, whole cell lysate.
(C) Bacterially purified His-G6PD protein was incubated with bacterially purified GST-CK2α or GST protein. GST pulldown was performed.
(D) Bacterially purified His-G6PD protein was incubated with bacterially purified GST-CK2α protein in the presence or absence of [γ-^{32}P]-ATP and/or CX-4945 for an *in vitro* kinase assay. Ni-NTA pulldown was performed, and radioactivity in the precipitates was measured by autoradiography.
(E) Alignment analyses of the flanking sequences of G6PD T76, T145 and T279 were performed among indicated species. T76, T145 and T279 were shown in red, and the necessary residues match CK2 phosphorylation consensus were shown in blue.
(F) Location of T76, T145 and T279, shown in purple, on human G6PD protein (PDB code: 6VAQ).
(G) Bacterially purified WT His-G6PD protein or indicated mutants were incubated with bacterially purified GST-CK2α protein in the presence ATPγS for an in *vitro* kinase assay. Ni-NTA pulldown was performed, and phosphorylation was determined using the thiophosphate ester (TE) specific antibody.
(H) HOK cells with expression of Flag-G6PD were treated with 12 Gy ionizing radiation. Immunoprecipitation was performed 30 min after irradiation, and immunoblots were then performed in the presence or absence of G6PD pT145 blocking peptide (ALPPpTVYEAVTKN).
(I) HOK and BEAS-2B cells with expression of WT Flag-G6PD or Flag-G6PD T145A were treated with 12 Gy ionizing radiation, and immunoprecipitation was performed 30 min after irradiation.
(J–K) BEAS-2B cells with expression of Flag-G6PD were pre-treated with 15 μM CX-4945 for 2 h (J) or expressed CK2α shRNA (K), and then treated with 12 Gy ionizing radiation. Immunoprecipitation was performed 30 min after irradiation. (For interpretation of the references to color in this figure legend, the reader is referred to the Web version of this article.)

in this assay to monitor the transfer of the phosphate group. Incubation with GST-CK2α protein caused an conspicuous autoradiographic band corresponding to His-G6PD protein, which was not detectable when GST-CK2α protein was not included in the system (Fig. 2D), suggesting that GST-CK2α phosphorylates His-G6PD with covalently linking the radioactive γ-phosphate group to His-G6PD. Further, phosphorylation of G6PD was not likely mediated by other contaminated kinases during G6PD or CK2α protein purification, as the autoradiographic band could be mostly erased when CX-4945 was used (Fig. 2D).

The consensus sequence of CK2 substrate contains a negatively charged glutamic acid (E) or aspartic acid (D) at position +3 downstream from the phosphorylation site (pS/T-x-x-D/E) [20]. Analysis of human G6PD protein sequence unveiled seven potential sites that match CK2 substrate consensus, including T_{76}VAD, T_{90}DEE, T_{145}VYE, T_{236}FKE, T_{279}NSD, S_{418}ELD, and T_{493}EAD. Among them, only T_{76}VAD, T_{145}VYE, and T_{279}NSD were conserved among multiple species (Fig. 2E) and

concurrently located on the protein surface (Fig. 2F). Replacement of these threonine sites with alanine (A) demonstrated that only T145A mutation countermanded CK2-mediated G6PD phosphorylation (Fig. 2G). To monitor this modification, an antibody recognized G6PD T145 phosphorylation was prepared and validated (Fig. 2H). With this antibody, G6PD T145 phosphorylation was found to be markedly accumulated in both HOK and BEAS-2B cells 30 min after exposure to 12 Gy ionizing radiation, which could be abolished by the non-phosphorylatable T145A mutation (Fig. 2I). As expected, this phosphorylation was also abated by the treatment of CX-4945 or CK2α shRNA (Fig. 2J–K). These results indicate that CK2 phosphorylates G6PD at T145 under ionizing radiation.

3.3. CK2-dependent T145 phosphorylation evokes G6PD enzymatic activity by facilitating G6PD interaction with $NADP^+$

Next, we studied the impact of CK2-dependent T145 phosphorylation on G6PD enzymatic activity. To introduce T145 phosphorylation on bacterially purified His-G6PD protein, His-G6PD protein was mixed with GST-CK2α protein in the presence of ATP for an *in vitro* kinase assay, and then purified by nickel-nitrilotriacetic acid (Ni-NTA) beads. We found that T145 phosphorylation consolidated G6PD enzymatic activity by approximately 6 folds (Fig. 3A). In contrast, the enzymatic activity of the nonphosphorylatable G6PD T145A mutant protein was comparable to that of WT G6PD protein, and stayed relatively unchanged after *in vitro* kinase assay, suggesting that CK2-dependent T145 phosphorylation elevated G6PD enzymatic activity (Fig. 3A). Consistently, ionizing radiation caused G6PD T145 phosphorylation companied with a conspicuous increase in G6PD enzymatic activity in both HOK and BEAS-2B cells, which could be obviously abrogated by T145A mutation (Fig. 3B).

G6PD reduces $NADP^+$ to NADPH by pulling two electrons from G6P and convert G6P into 6-phosphogluconolactone [21]. Inspection of the reported human G6PD protein structures indicated that T145 site is spatially located within the G6PD catalytic domain (Fig. 3C). Further, analysis of the G6PD-substrate binding mode, based on the co-crystallization of G6PD with $NADP^+$ (PDB code: 6VAQ) or G6P (PDB code: 5UKW), discovered that T145 site is close to $NADP^+$-binding site, whereas distant to G6P-binding site (Fig. 3C). This finding prompted us to test whether T145 phosphorylation increased G6PD enzymatic activity by modulating the interaction between G6PD and $NADP^+$. T145-phosphorylated His-G6PD protein was prepared by CK2α-dependent *in vitro* kinase assay, and its binding affinity with $NADP^+$ was measured by using [^{14}C]-$NADP^+$. As expected, compared to the unphosphorylated counterparts, G6PD protein bearing T145 phosphorylation showed higher binding affinity with $NADP^+$, evidenced by the markedly increased radioactive signal in the His-G6PD precipitates

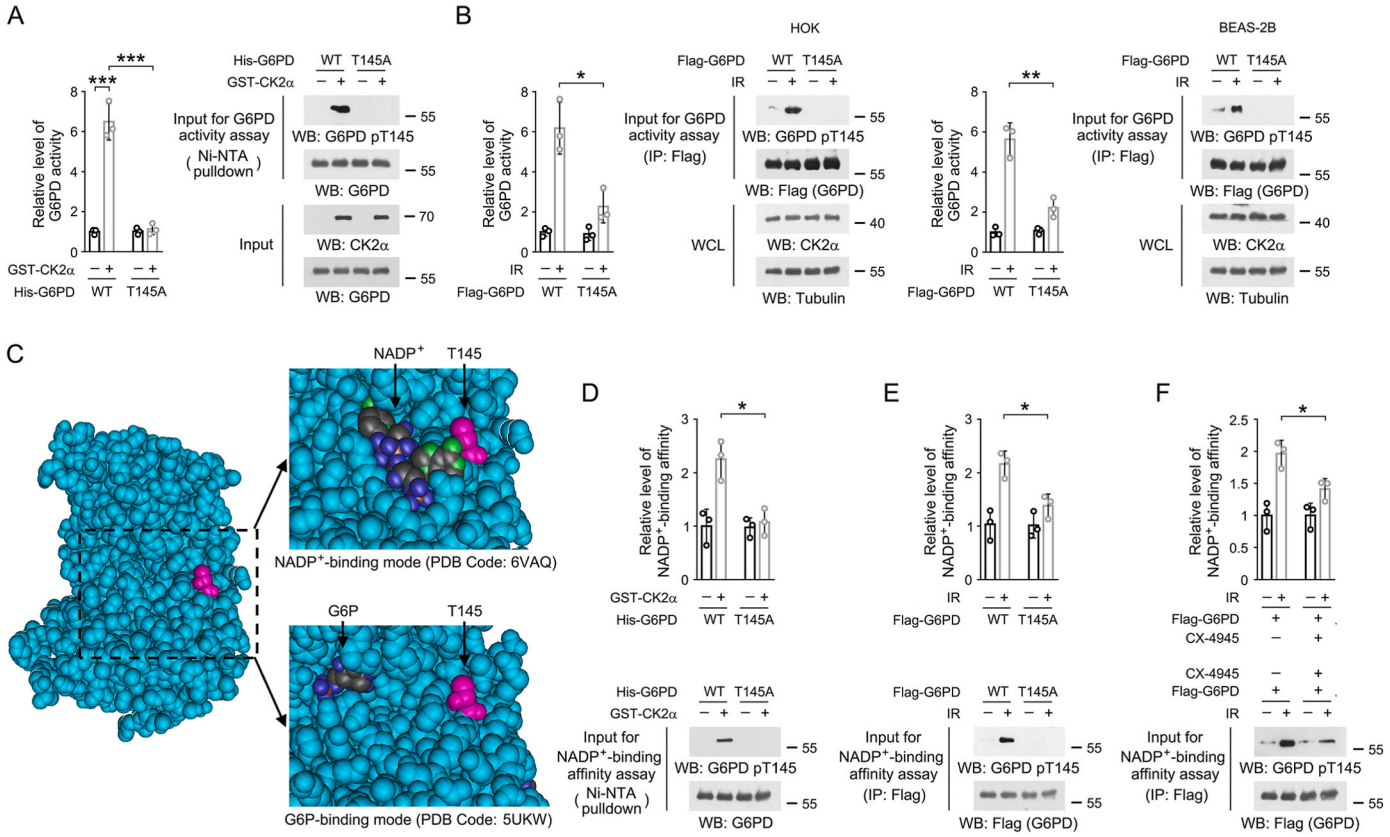

Fig. 3. CK2-dependent T145 phosphorylation activates G6PD by facilitating G6PD binding with $NADP^+$ (A) Bacterially purified WT His-G6PD or T145A mutant protein was incubated with purified GST-CK2α proteins for an *in vitro* kinase assay. Ni-NTA pulldown was performed, and the G6PD enzymatic activity in the precipitates was measured. $^{***}P < 0.001$. (B) HOK and BEAS-2B cells with expression of WT Flag-G6PD or Flag-G6PD T145A were treated with 12 Gy ionizing radiation. Flag-G6PD proteins were precipitated from cell lysates 30 min after irradiation, and the G6PD enzymatic activity in the precipitates was measured. IR, ionizing radiation; WCL, whole cell lysate; $^{*}P < 0.05$, $^{**}P < 0.01$. (C) The catalytic domain of human G6PD protein was boxed and T145 was shown in purple (left panel). The $NADP^+$-binding mode (PDB code: 6VAQ) and G6P-binding mode (PDB code: 5UKW) were shown. (D) Bacterially purified WT His-G6PD or T145 mutant protein was incubated with purified GST-CK2α for an *in vitro* kinase assay. Ni-NTA pulldown was performed, and the binding affinity between G6PD protein and $NADP^+$ was measured. $^{*}P < 0.05$. (E) HOK cells with expression of WT Flag-G6PD or Flag-G6PD T145A were treated with 12 Gy ionizing radiation. Flag-G6PD proteins were precipitated from cell lysates 30 min after irradiation, washed twice with PBS, and the binding affinity between G6PD protein and $NADP^+$ was measured. $^{*}P < 0.05$. (F) HOK cells with expression of WT Flag-G6PD were pre-treated with 15 μM CX-4945C for 2 h, and cells were then treated with 12 Gy ionizing radiation. Flag-G6PD proteins were precipitated from cell lysates 30 min after irradiation, washed twice with PBS, and the binding affinity between G6PD protein and NADP was measured. $^{*}P < 0.05$. (For interpretation of the references to color in this figure legend, the reader is referred to the Web version of this article.)

(Fig. 3D). Similar effects were also observed in the Flag-G6PD protein purified from irradiated HOK cells (Fig. 3E). Further, this T145 phosphorylation-facilitated G6PD/$NADP^+$ association could be largely abolished by T145A mutation or treatment with CX-4945 (Fig. 3D–F). These results suggest that CK2-mediated T145 phosphorylation activates G6PD by promoting its binding with $NADP^+$.

3.4. G6PD T145 phosphorylation is required for maintaining redox homeostasis and support cell proliferation upon ionizing radiation

Next, we sought to determine the impact of CK2-mediated G6PD T145 phosphorylation on ionizing radiation-induced oxidative stress. To this end, expression of endogenous G6PD in HOK or BEAS-2B cells was knocked down by shRNA that targeted the non-coding region of G6PD mRNA, and nearly equal amount of Flag-tagged WT G6PD or G6PD T145A mutant was exogenously expressed (Fig. 4A). As expected, ionizing radiation induced palpable G6PD T145 phosphorylation in cell with WT Flag-G6PD but not the mutant one (Fig. 4B). Notably, ionizing radiation-diminished cellular NADPH pool further shrunk in both HOK and BEAS-2B cells expressing G6PD T145A (Fig. 4C). In contrast, G6PD T145A mutation had minor effects on cellular NADPH level in the untreated cells (Fig. 4C), which was in accordance with our finding that G6PD T145A mutation did not affect the basal activity of G6PD (Fig. 3A–B). G6PD governs the rate-limiting step of PPP that shunts the carbon flux from glycolysis to PPP (Fig. 4D) [6]. As expected, ionizing radiation resulted in an evident accumulation of cellular ^{14}C-labeled R5P, the final product of PPP, after incubation with ^{14}C-labeled glucose (Fig. 4E). However, ionizing radiation-induced R5P synthesis from

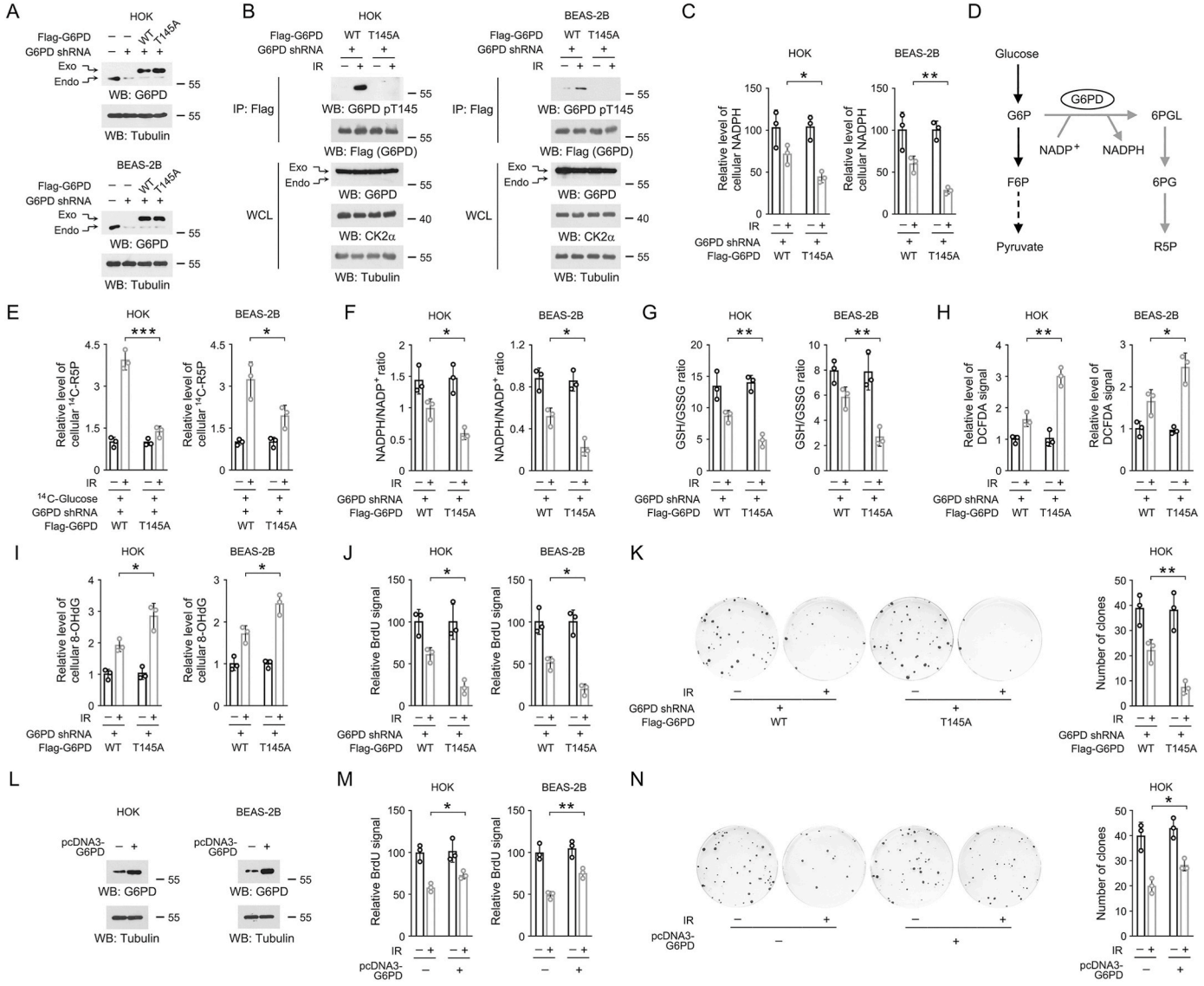

Fig. 4. G6PD T145 phosphorylation is required for maintaining redox homeostasis and support cell proliferation under ionizing radiation

(A-C, E-K) Endogenous G6PD-depleted HOK or BEAS-2B cells were stably expressed with WT Flag-G6PD or Flag-G6PD T145A (A). Cells were treated with 12 Gy ionizing radiation (B). Cellular NADPH level (C), NADPH/$NADP^+$ ratio (F), GSH/GSSG ratio (G), DCFDA level (H), 8-OHdG level (I) was measured 3 h after irradiation. Cells were incubated with D-[6–^{14}C] glucose (1 μCi, 0.01 mmol/L) for 1 h after irradiation, and the level of ^{14}C–R5P was measured (E). Cell proliferation was measured by BrdU incorporation assay (J) or colony formation assay (K, HOK cells). IR, ionizing radiation; WCL, whole cell lysate; $^*P < 0.05$; $^{**}P < 0.01$; $^{***}P < 0.001$.

(D) A schematic of glycolysis pathway and PPP. 6PGL, 6-phosphogluconolactone; F6P, fructose-6-phosphate; 6 PG, 6-phosphogluconate.

(L–M) HOK and BEAS-2B cells were stably expressed with or without pcDNA3-G6PD vector, and expression of G6PD was examined by immunoblot (L). Cells were treated with 12 Gy ionizing radiation, and cell proliferation was measured by BrdU incorporation assay (M) or colony formation assay (N, HOK cells). $^*P < 0.05$; $^{**}P < 0.01$.

glucose was substantially abolished in those cells with G6PD T145A (Fig. 4E). These results suggest that G6PD T145 phosphorylation was required for maintaining NADPH pool and evoking PPP under ionizing radiation.

NADPH is an essential component of antioxidant defenses mainly through reduction of oxidized GSH [22]. Indeed, though no obvious difference was found for unirradiated cells, apparently lowed values of both NADPH/$NADP^+$ radio and GSH/GSSG radio were observed in G6PD T145A mutant-expressed HOK and BEAS-2B cells, compared to the WT counterparts after exposure to ionizing radiation (Fig. 4F–G). Additionally, a more intense 2,7-Dichlorofluoroscin Diacetate (DCFDA) and 8-hydroxydeoxyguanosine (8-OHdG) signal was detected in the cells expressing G6PD T145A under ionizing radiation, hinting a higher level of cellular ROS and guanosine oxidation-based DNA damage, respectively (Fig. 4H–I). Further, evidenced by Bromodeoxyuridine (BrdU) cell proliferation assay (Fig. 4J) and colony formation assay (Fig. 4K), the proliferation rate was comparable for unirradiated cells regardless whether WT G6PD or G6PD T145A was expressed. Remarkably, though the proliferative capacity was repressed in both WT and mutant cells upon ionizing radiation, it declined to a conspicuously lower level in the G6PD T145A-epxressed cells (Fig. 4J–K). In line with this, overexpression of G6PD partially restored the proliferation rate in the irradiated cells, though no obvious effects were found in the unirradiated cells (Fig. 4L–N). These results suggest that CK2-dependent G6PD T145 phosphorylation is required for maintaining redox homeostasis and support cell proliferation under ionizing radiation.

4. Discussion

Treatment with ionizing radiation results in massive oxidizing events in a living cell that modulate atomic structure by the interactions of target macromolecules with electromagnetic waves or subatomic particles [3]. Particularly, ionizing radiation-induced radiolysis of cytosolic water leads to the exceedingly rapid generation of various reactive molecules, with initial rupture of oxygen-hydrogen, nitrogen-hydrogen, and carbon-hydrogen bonds within 10^{-14}~10^{-12} s, and subsequent oxidative damages of cellular macromolecules within 10^{-12} s [3]. In our result, increased cellular G6P dehydrogenation activity was detected 30 min after ionizing radiation in both HOK and BEAS-2B cells. Further, G6PD binding with CK2 and phosphorylation of G6PD T145 could be also detected within 30 min after ionizing radiation, indicating that G6PD activation is a rapid response to ionizing radiation. It is documented that G6PD expression could be upregulated after cells were exposed to multiple oxidative stress-inducing stimuli for more than 12 h [23]. In contrast, our data show that G6PD expression was largely unchanged within 90 min after 12 Gy ionizing radiation, suggesting that the enhanced cellular G6P dehydrogenation activity was resulted from the increase in G6PD enzymatic activity rather than its protein expression. Therefore, the present data reports a new protein modification-dependent mechanism, through which cells rapidly cope with ionizing radiation-induced oxidative stress by consolidating G6PD-dependent NADPH production.

CK2 is a conserved pleiotropic and constitutively activated serine/threonine protein kinase that ubiquitously exists in all eukaryotes. As one of the firstly identified protein kinases, CK2 can phosphorylate more than three hundred protein substrates, and so that has crucial impact on diverse cell life activities, controlling a variety of metabolic processes [19]. CK2 has been widely established as an essential regulator in the context of ionizing radiation. In human cervical cancer cells, CK2α subunit accumulated in the nucleus after ionizing radiation, and inhibited apoptosis by negatively modulating the endoproteolytic activity of Caspases, in a manner independent of other CK2 subunits [24]. Additionally, the radiosensitivity of non-small-cell lung cancer cells was increased when cells were treated with CK2-specific siRNA [25]. Further, CK2 was found to protect mesenchymal stem cells from ionizing radiation-elicited senescence, probably through regulating cytoskeleton reorganization [18]. In this study, we demonstrate that evolutionally conserved G6PD T145 site, whose flanking sequence matches the canonical CK2 phosphorylation consensus, is a new CK2 phosphorylation substrate. By using bacterially purified G6PD and CK2α proteins, we established an *in vitro* kinase assay and showed that CK2α directly phosphorylated G6PD using ATP as a phosphate group donor, which could be largely abolished by CK2 inhibitor CX-4945 or G6PD T145A mutation. Therefore, the present data broadens the knowledge of the role of CK2 in the signal transduction under ionizing radiation. As mammalian CK2 is a homomeric or heteromeric complex consisting of two regulatory β subunits, which controls substrate selectivity and maintain enzyme stability, and two catalytic α subunits [26], more work is required to decipher the specific role of each CK2 subunit in the regulation of G6PD.

Recently, CK2 kinase has been considered as a promising radiosensitizing agent in tumor treatment. It is documented that the cytotoxic effect of irradiation in non-small cell lung cancer (NSCLC) cells could be augmented by 4,5,6,7-Tetrabromo-1H-benzotriazole (TBB) and Tetrabromocinnamic acid (TBCA), two CK2 inhibitors, which was associated with the suppression of Stat3 activation [27]. Treatment with Quinalizarin and CX-4945, another two CK2 inhibitors, abrogated endothelial cell-elicited production of cytokines and formation of a perivascular resistant niche, thereby sensitizing NSCLC cells to radiotherapy [28]. In addition, treatment with the combination of ionizing radiation and Quinalizarin resulted in a delay in the repair of DNA double-strand breaks, arrest of G2/M checkpoint and increased apoptosis in NSCLC cells, compared to the tumor cells treated with only ionizing radiation [25]. Considering the data presented in this study, it is noteworthy that the use of CK2 inhibitors may counteract with CK2-dependent G6PD T145 phosphorylation and NADPH production, thereby accentuating radiation-induced damages in normal tissues. Therefore, to limit the potential side effects of CK2 inhibitors during tumor radiotherapy, further work is need to develop the suitable tumor-targeting delivery strategies for CK2 inhibitors.

PPP is a major branch of glycolysis, and the rate-limiting enzyme of this metabolic route, G6PD, contributes to a large proportion of the cellular NADPH production [6]. G6PD overexpression transgenic mice has higher levels of NADPH, reduced levels of oxidative stress-induced damages, and prolonged lifespan; in contrast, knockout of this gene is embryonic lethal for mice [29,30]. G6PD deficiency is a common genetic defect with more than 400 million people diagnosed worldwide, which can result in ROS accumulation and cause multitudinous diseases, such as hemolysis and neurodegeneration [31]. G6PD-deficient nucleated cells are more susceptible to oxidative stress-induced cell death due to inadequate GSH [32]. Consistently, we demonstrate here that CK2-dependent G6PD T145 phosphorylation was required to reinforce the metabolic flux of PPP and contributed to maintain the cellular NADPH level in both the irradiated HOK and BEAS-2B cells. A non-phosphorylatable G6PD T145A mutation accentuated ionizing radiation-induced oxidative stress, including the decreased radio of NADPH/$NADP^+$ and GSH/GSSG, and the enhanced DCFDA and 8-OHdG signal, and the further impaired cell proliferation. Therefore, our results indicate that CK2-mediated phosphorylation and activation of G6PD promotes anti-oxidative defense and support cell proliferation under ionizing radiation.

NADPH is vital for living cells as it provides the universal reducing power that fuels the anti-oxidative enzymes for recycling the oxidized glutathione [22]. In the present study, we report a novel G6PD-associated anti-oxidative defense mechanism under ionizing radiation (Fig. 5). CK2-mediated phosphorylation and activation of G6PD boosts NADPH synthesis to support cellular redox homeostasis, highlighting its potential value in the early treatment of ionizing radiation-induced injuries.

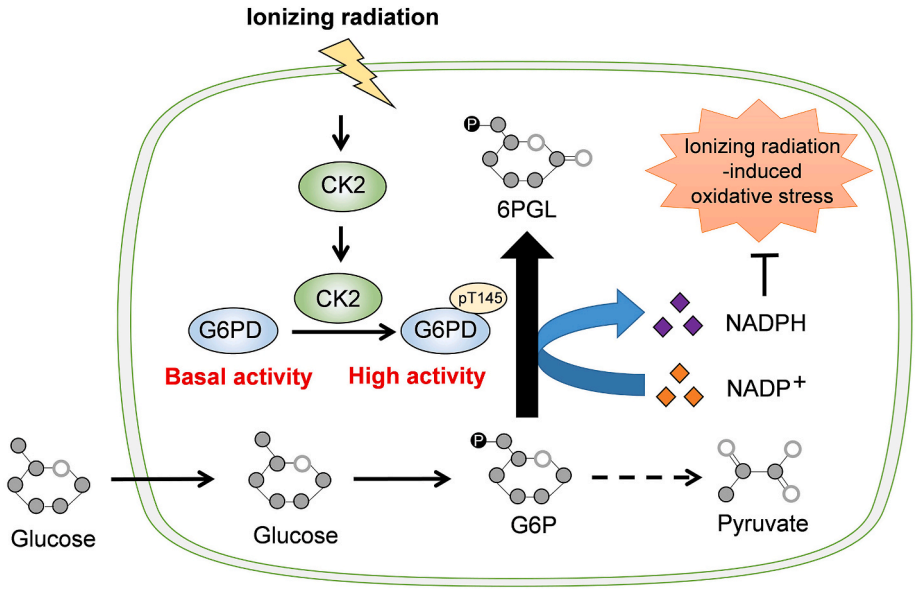

Fig. 5. A schematic of CK2-mediated G6PD activation under ionizing radiation Ionizing radiation rapidly induces G6PD binding with CK2, leading to CK2-dependent G6PD T145 phosphorylation, which increases G6PD enzymatic activity and enhances NADPH production, thereby facilitating cell proliferation by maintaining cellular redox homeostasis. 6PGL, 6-phosphogluconolactone.

5. Conclusions

Radiation-induced oral mucositis and pneumonitis are the most common complications for the patients who receive radiotherapy, and the development of both complications is companied with oxidative stress and multiple temporary or irreversible damages in the irradiated tissues. The metabolic routes for nucleotide production not only provide the building blocks for DNA/RNA synthesis, but also act as the major source to generate NADPH. The current data leads to a better understanding of how nucleotide metabolism can be rapidly modulated in response to ionizing radiation by post-translational modification of enzymes, and adds to the knowledge of the regulatory mechanisms of cellular redox homeostasis.

Authors' contributions

Conceptualization: Q.C., R.L., and Q.T.; methodology: Y.H., X.H., M.L., and J.L.; investigation: Y.H., X.H., M.L., and J.L.; writing (original draft): R.L.; writing (review and editing): R.L.; funding acquisition: Q.C., R.L., and Y.H. All authors read and approved the final manuscript.

Declaration of competing interest

The authors declare that they have no known competing financial interests or personal relationships that could have appeared to influence the work reported in this paper.

Data availability

Data will be made available on request.

Acknowledgements

This work was supported by Sichuan Science and Technology Program 2023NSFSC1924 (R.L.), National Natural Science Foundation of China grants 82001047 (Y.H.), Zhejiang Provincial Key Research and Development Program 2021C03074 (Q.C.), Zhejiang Provincial Medical Health Major Science Program WKJ-ZJ-2212 (Q.C.), and the Science Foundation of West China Hospital of Stomatology RCDWJS2023-2 (R.L.).

References

[1] M.H. Barcellos-Hoff, C. Park, E.G. Wright, Radiation and the microenvironment - tumorigenesis and therapy, Nat. Rev. Cancer 5 (11) (2005) 867–875.
[2] E.I. Azzam, J.P. Jay-Gerin, D. Pain, Ionizing radiation-induced metabolic oxidative stress and prolonged cell injury, Cancer Lett. 327 (1–2) (2012) 48–60.
[3] J.A. Reisz, N. Bansal, J. Qian, W. Zhao, C.M. Furdui, Effects of ionizing radiation on biological molecules–mechanisms of damage and emerging methods of detection, Antioxidants Redox Signal. 21 (2) (2014) 260–292.
[4] G.R. Drummond, S. Selemidis, K.K. Griendling, C.G. Sobey, Combating oxidative stress in vascular disease: NADPH oxidases as therapeutic targets, Nat. Rev. Drug Discov. 10 (6) (2011) 453–471.
[5] H.J. Forman, H. Zhang, Targeting oxidative stress in disease: promise and limitations of antioxidant therapy, Nat. Rev. Drug Discov. 20 (9) (2021) 689–709.
[6] K.C. Patra, N. Hay, The pentose phosphate pathway and cancer, Trends Biochem. Sci. 39 (8) (2014) 347–354.
[7] E.C. Britt, J. Lika, M.A. Giese, T.J. Schoen, G.L. Seim, Z. Huang, et al., Switching to the cyclic pentose phosphate pathway powers the oxidative burst in activated neutrophils, Nature metabolism 4 (3) (2022) 389–403.
[8] A.A. Garcia, A. Koperniku, J.C.B. Ferreira, D. Mochly-Rosen, Treatment strategies for glucose-6-phosphate dehydrogenase deficiency: past and future perspectives, Trends Pharmacol. Sci. 42 (10) (2021) 829–844.
[9] L. Chen, Z. Zhang, A. Hoshino, H.D. Zheng, M. Morley, Z. Arany, et al., NADPH production by the oxidative pentose-phosphate pathway supports folate metabolism, Nature metabolism 1 (2019) 404–415.
[10] J. Li, T. Zhang, T. Ren, X. Liao, Y. Hao, J.S. Lim, et al., Oxygen-sensitive methylation of ULK1 is required for hypoxia-induced autophagy, Nat. Commun. 13 (1) (2022) 1172.
[11] J. Li, J. Shao, Z. Zeng, Y. He, C. Tang, S.H. Park, et al., Mechanosensitive turnover of phosphoribosyl pyrophosphate synthetases regulates nucleotide metabolism, Cell Death Differ. 29 (1) (2022) 206–217.
[12] L. An, P. Nie, M. Chen, Y. Tang, H. Zhang, J. Guan, et al., MST4 kinase suppresses gastric tumorigenesis by limiting YAP activation via a non-canonical pathway, J. Exp. Med. 217 (6) (2020).
[13] G.F. Gaetani, A.M. Ferraris, P. Sanna, H.N. Kirkman, A novel NADPH:(bound) NADP+ reductase and NADH:(bound) NADP+ transhydrogenase function in bovine liver catalase, Biochem. J. 385 (Pt 3) (2005) 763–768.
[14] M.A. Becker, Patterns of phosphoribosylpyrophosphate and ribose-5-phosphate concentration and generation in fibroblasts from patients with gout and purine overproduction, J. Clin. Invest. 57 (2) (1976) 308–318.
[15] R. Liu, J. Li, J. Shao, J.H. Lee, X. Qiu, Y. Xiao, et al., Innate immune response orchestrates phosphoribosyl pyrophosphate synthetases to support DNA repair, Cell Metabol. 33 (10) (2021) 2076–2089.e2079.
[16] S.C. Liu, C.M. Huang, Y.L. Chang, O.A. Bamodu, C.T. Yeh, H.W. Wang, et al., Ovatodiolide suppresses inflammatory response in BEAS-2B cells by regulating the CREB/AQP5 pathway, and sensitizes nasopharyngeal carcinoma cells to radiation therapy, Eur. J. Pharmacol. 859 (2019), 172548.
[17] J. Pi, Y. Bai, J.M. Reece, J. Williams, D. Liu, M.L. Freeman, et al., Molecular mechanism of human Nrf2 activation and degradation: role of sequential phosphorylation by protein kinase CK2, Free Radical Biol. Med. 42 (12) (2007) 1797–1806.

[18] D. Wang, D.J. Jang, Protein kinase CK2 regulates cytoskeletal reorganization during ionizing radiation-induced senescence of human mesenchymal stem cells, Cancer Res. 69 (20) (2009) 8200–8207.
[19] C. Borgo, C. D'Amore, S. Sarno, M. Salvi, M. Ruzzene, Protein kinase CK2: a potential therapeutic target for diverse human diseases, Signal Transduct. Targeted Ther. 6 (1) (2021) 183.
[20] C. Franchin, C. Borgo, L. Cesaro, S. Zaramella, J. Vilardell, M. Salvi, et al., Re-evaluation of protein kinase CK2 pleiotropy: new insights provided by a phosphoproteomics analysis of CK2 knockout cells, Cell. Mol. Life Sci. : CMLS 75 (11) (2018) 2011–2026.
[21] X. Wei, K. Kixmoeller, E. Baltrusaitis, X. Yang, R. Marmorstein, Allosteric role of a structural NADP(+) molecule in glucose-6-phosphate dehydrogenase activity, Proc. Natl. Acad. Sci. U. S. A. 119 (29) (2022), e2119695119.
[22] H.Q. Ju, J.F. Lin, T. Tian, D. Xie, R.H. Xu, NADPH homeostasis in cancer: functions, mechanisms and therapeutic implications, Signal Transduct. Targeted Ther. 5 (1) (2020) 231.
[23] Y. Zhang, Y. Xu, W. Lu, J. Li, S. Yu, E.J. Brown, et al., G6PD-mediated increase in de novo NADP(+) biosynthesis promotes antioxidant defense and tumor metastasis, Sci. Adv. 8 (29) (2022), eabo0404.
[24] K. Yamane, T.J. Kinsella, CK2 inhibits apoptosis and changes its cellular localization following ionizing radiation, Cancer Res. 65 (10) (2005) 4362–4367.
[25] Q. Li, K. Li, T. Yang, S. Zhang, Y. Zhou, Z. Li, et al., Association of protein kinase CK2 inhibition with cellular radiosensitivity of non-small cell lung cancer, Sci. Rep. 7 (1) (2017), 16134.
[26] L. Herhaus, A.B. Perez-Oliva, G. Cozza, R. Gourlay, S. Weidlich, D.G. Campbell, et al., Casein kinase 2 (CK2) phosphorylates the deubiquitylase OTUB1 at Ser16 to trigger its nuclear localization, Sci. Signal. 8 (372) (2015) ra35.
[27] Y.C. Lin, M.S. Hung, C.K. Lin, J.M. Li, K.D. Lee, Y.C. Li, et al., CK2 inhibitors enhance the radiosensitivity of human non-small cell lung cancer cells through inhibition of stat3 activation, Cancer Biother. Radiopharm. 26 (3) (2011) 381–388.
[28] Q. Li, Y. Zong, K. Li, X. Jie, J. Hong, X. Zhou, et al., Involvement of endothelial CK2 in the radiation induced perivascular resistant niche (PVRN) and the induction of radioresistance for non-small cell lung cancer (NSCLC) cells, Biol. Res. 52 (1) (2019) 22.
[29] S. Nóbrega-Pereira, P.J. Fernandez-Marcos, T. Brioche, M.C. Gomez-Cabrera, A. Salvador-Pascual, J.M. Flores, et al., G6PD protects from oxidative damage and improves healthspan in mice, Nat. Commun. 7 (2016), 10894.
[30] L. Longo, O.C. Vanegas, M. Patel, V. Rosti, H. Li, J. Waka, et al., Maternally transmitted severe glucose 6-phosphate dehydrogenase deficiency is an embryonic lethal, EMBO J. 21 (16) (2002) 4229–4239.
[31] E. Theodorsson, H. Birgens, T.A. Hagve, Haemoglobinopathies and glucose-6-phosphate dehydrogenase deficiency in a Scandinavian perspective, Scand. J. Clin. Lab. Investig. 67 (1) (2007) 3–10.
[32] T. Efferth, S.M. Schwarzl, J. Smith, R. Osieka, Role of glucose-6-phosphate dehydrogenase for oxidative stress and apoptosis, Cell Death Differ. 13 (3) (2006) 527–528, author reply 529-530.